

Millennial-scale climate changes manifest Milankovitch combination tones and Hallstatt solar cycles in the Devonian greenhouse world

A.C. Da Silva^{1,2*}, M.J. Dekkers², D. De Vleeschouwer³, J. Hladil⁴, L. Chadimova⁴, L. Slavík⁴, and F.J. Hilgen²

¹Sedimentary Petrology Laboratory, Liège University, 4000 Liège, Belgium

²Department of Earth Sciences, Utrecht University, PO Box 80125, 3508 TC Utrecht, Netherlands

³MARUM—Zentrum für Marine Umweltwissenschaften, Universität Bremen, 28359 Bremen, Germany

⁴Institute of Geology of the Czech Academy of Sciences, CZ-165 00 Prague 6 – Lysolaje, Czech Republic

ABSTRACT

Sub-Milankovitch rhythmic features in sedimentary records have been reported from throughout geological time. However, their origin remains enigmatic, in particular during so-called greenhouse periods in Earth's history. To better understand such short-term climatic changes, we sampled two 3-m-thick intervals of early Devonian hemipelagic carbonate at 1 cm resolution in the Pod Barrandovem section (Czech Republic). Greenhouse conditions prevailed during early Devonian times, and the chosen resolution enables the detection of millennial-scale climate change as recorded by elemental abundances. We used a previously published astrochronology for the section to transform the studied series from the stratigraphic into the time domain. Spectral analysis of the time-calibrated log-transformed Ti records reveal obliquity and precession cycles, confirming the applied astrochronology. Additional spectral peaks with periods of 2.3–2.7, 6–8, and 10–12 k.y. appear in both records. Furthermore, a 1.5 k.y. periodicity, close to the Pleistocene Dansgaard-Oeschger oscillation, is also identified, but only in the record with higher accumulation rate (~3.5 cm/k.y.). Bi-coherence spectra reveal that the 6–8 and 10–12 k.y. periodic components are combination tones of Milankovitch cycles. We infer the shorter ~2.5 k.y. periodicity to be the result of solar forcing, related to the Hallstatt cycle. These new observations strengthen the case for an external origin of millennial-scale features.

INTRODUCTION

Periodic climate changes at the millennial scale (shorter than precession and longer than 1 k.y.) have been extensively studied. They are best known from the late Pleistocene and include Dansgaard-Oeschger oscillations (~1.5 k.y.; Dansgaard et al., 1989) and Heinrich events (5–10 k.y.; Heinrich, 1988). The occurrence of these periodic climate changes is interpreted to be related to internal mechanisms, such as ice sheet dynamics or ocean-atmosphere system variations (e.g., MacAyeal, 1993; Alley et al., 1999), or to external mechanisms, such as solar forcing (e.g., Braun et al., 2005) or nonlinear signal transformation producing harmonics and/or intermodulation frequencies of primary orbital (Milankovitch) cycles (von Döbenek and Schmieder, 1999; Wara et al., 2000; Berger et al., 2006). Millennial-scale climate variations have also been identified in older and commonly much warmer intervals of Earth's history. Here, we document

millennial-scale climate variations archived in two 3-m-long portions of a lower Devonian greenhouse succession from the Czech Republic (Pod Barrandovem section, Prague synform) with the aim of further substantiating their persistent existence, thus contributing to solving their enigmatic origin. Elemental geochemistry (portable X-ray fluorescence, XRF) was measured every centimeter, and an existing astrochronology for the section (Da Silva et al., 2016) was used to transform the two newly sampled portions from the stratigraphic domain into the time domain. Time-series analysis of these time-domain log(Ti) records enables us to identify the duration of millennial-scale quasi-periods, while bi-coherence spectra allow the detection of potential nonlinear coupling of different frequencies.

GEOLOGICAL SETTING

The Devonian was a globally warm period (Joachimski et al., 2009). Yet, the Lochkovian-Pragian transition is marked by rapid cooling, followed by a renewed warming in the Pragian. This warming led to relatively hot, unstable, and humid climatic conditions. However, by the late Pragian and early Emsian, global climate had become cooler again (Slavík et al., 2016). Here, we focus on the Praha Formation, a record of the Pragian to Emsian in the Prague synform, dominated by distal offshore carbonate facies, mostly hemipelagites and calciturbidites (Hladil et al., 2010). The Pod Barrandovem section was located at 20°–35°S paleolatitude during the early Devonian (Fig. DR1 in the GSA Data Repository¹). The Praha Formation portion of the Pod Barrandovem section is ~180 m thick and comprises ~10-cm-thick carbonate beds with slightly clayey offshore limestones. The cyclostratigraphic study of Da Silva et al. (2016) of the Praha Formation at Pod Barrandovem is based on magnetic susceptibility and gamma ray spectrometry records. The astrochronologic age model developed for the succession indicates that precession cycles are ~1 m thick throughout most of the section (Da Silva et al., 2016). In other words, the ~10-cm-thick bedding is one-order-of-magnitude thinner than the sedimentary expression of the Milankovitch-band astronomical cycles.

We selected two intervals in the 180-m-thick section (Fig. DR1), with different sedimentation rates and ages. The Pragian interval 1 (9.7–12 m)

¹GSA Data Repository item 2019005, Figures DR1 and DR2, and original log-transformed Ti data from interval 1 (Pragian) (File DR1) and from interval 2 (Emsian) (File DR2), is available online at <http://www.geosociety.org/datarepository/2019/> or on request from editing@geosociety.org.

*E-mail: ac.dasilva@uliege.be

CITATION: Da Silva, A.C., et al., 2018, Millennial-scale climate changes manifest Milankovitch combination tones and Hallstatt solar cycles in the Devonian greenhouse world: *Geology*, v. 47, p. 19–22, <https://doi.org/10.1130/G45511.1>.

is a greenish clayey laminated limestone (Chlupáč, 2000), while the Emsian interval 2 (124.7–127.7 m) consists of micritic beds and carbonate beds with higher clay contents and nodular interbeds (Chlupáč, 2000).

METHODOLOGY

Samples from both intervals were collected at 1 cm resolution, with successive samples having some stratigraphic overlap. This sampling strategy assumes a continuous stratigraphic recovery of the studied intervals. Rock samples were cut in half to measure XRF elemental geochemistry (major and trace) on a clean surface. As both intervals are ~3 m thick, we carried out a total number of ~300 measurements per interval. XRF measurements were conducted under laboratory conditions, using a Thermo Scientific Niton XL3t SDD (900 GOLDD) Series portable XRF analyzer, with a steady flow of helium (at Utrecht University, Netherlands). Each XRF point measurement is the average of two to five measurements, depending on their stability, with good stability being <5% difference between repeated measurements (for Ti; counting time of 80 s). We have selected the element Ti for our study because it is a good proxy for detrital input, is a relatively immobile element, and is not very sensitive to diagenetic processes (e.g., MacLean et al., 1997). Spectral techniques were then applied to the tuned log(Ti) record. By using the logarithmic signal, modest base-level variations are enhanced while positive peak values are reduced.

The sedimentation rate estimates are 1.5 cm/k.y. for interval 1 and 3.5 cm/k.y. for interval 2 (Da Silva et al., 2016). We used these sedimentation rates to transform the log(Ti) records from the stratigraphic domain into the time domain (Fig. DR2). Following interpolation, detrending, and time calibration, we applied multitaper method (MTM) spectral analysis, a MTM harmonic test (F-test; Thomson, 1982), and bandpass filtering of the log(Ti) using the “astrochron” R package developed by Meyers (2014).

We also applied continuous wavelet transform (CWT, Morlet waveform; Torrence and Compo, 1998) to track the evolution of the frequency of the main spectral peaks through time. The bi-coherence spectrum (Hagelberg et al., 1991) was calculated with a MatLab script by Du (2013) from the MatLab Higher Order Spectral Analysis (HOSA) toolbox. Bi-coherence spectral analysis allows detection of nonlinear coupling of different frequencies (Hagelberg et al., 1991), where the nonlinear inter-modulation of two frequencies f_1 and f_2 generates a third frequency f_3 , a combination of f_1 and f_2 . On bi-coherence spectra, such combination tones are expressed by a spectral maximum (corresponding in our color coding to a red spot) at the junction of the two frequencies (with f_1 and f_2 plotted as x -axis and y -axis, respectively).

RESULTS

The CWTs of the two time-domain series (Fig. 1) reveal marked power bands around 16–19 k.y. and ~31 k.y., in agreement with the anticipated periods of precession and obliquity at that time (Berger et al., 1992). The CWT spectra of the two intervals show further elevated spectral power bands at periods of 6–8 and 10–12 k.y. (Fig. 1). The MTM spectra and F-tests of the two time series also show a number of significant peaks at frequencies higher than that of the primary Milankovitch cycles, corresponding to periods of 1.3–1.7, 2.3–2.7, 6–8, and 10–12 k.y. (Fig. 1).

Although the two studied intervals are separated by several million years (Da Silva et al., 2016), both intervals exhibit similar millennial-scale periodicities in log(Ti). We further investigated whether these variations correspond to persistent periodic changes in the two time series or reflect artifacts by applying bandpass filters centered at the relevant frequencies (extracted from the MTM spectra) and by comparing the filtered components with the log(Ti) time series (see also de Winter et al., 2014). Misfits

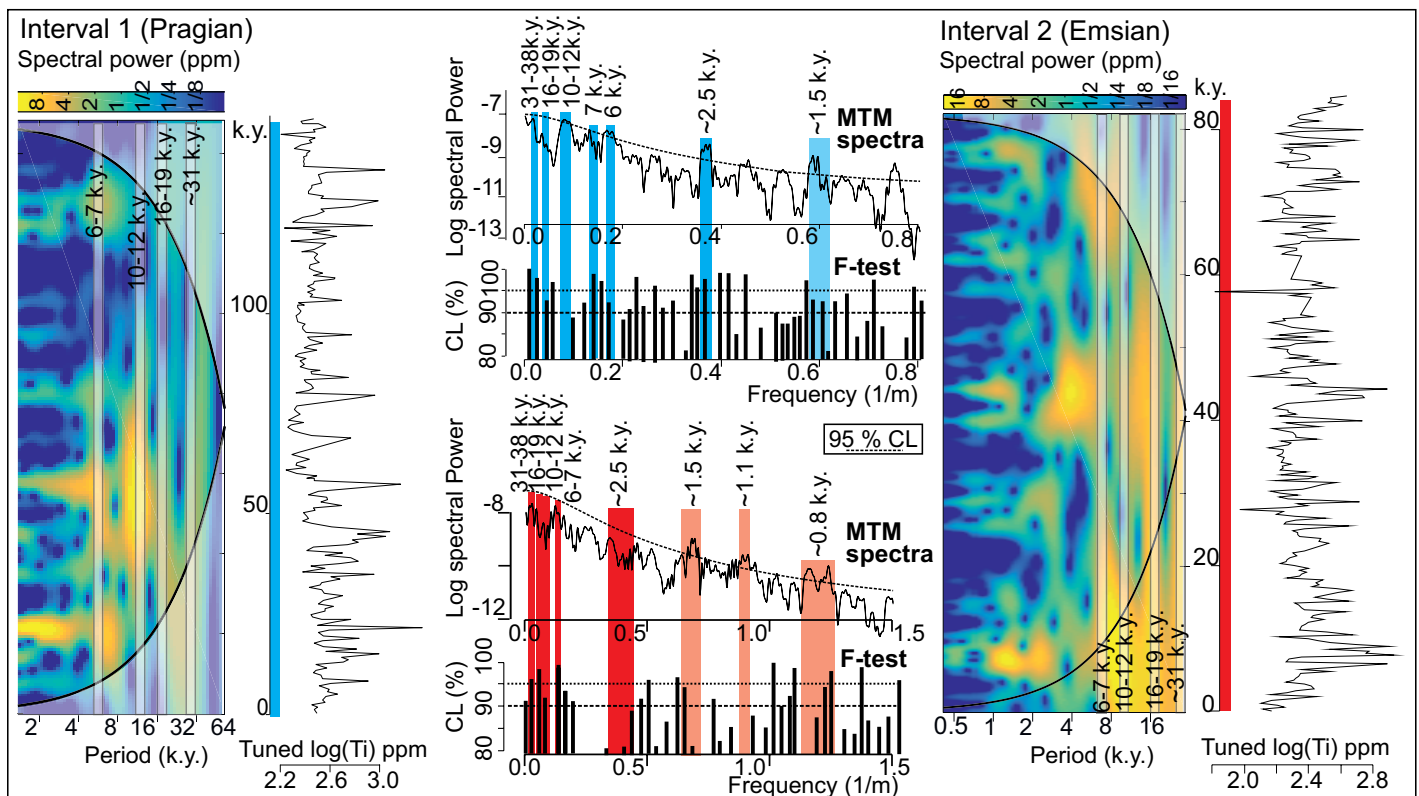


Figure 1. Log(Ti) concentration in time domain from interval 1 and interval 2 from Pragian and Emsian parts, respectively of Pod Barrandovem section (Czech Republic) and respective spectral analysis, including continuous wavelet transform and multitaper method (MTM) spectra and F-tests (two tapers) of tuned log(Ti) records (with 95% confidence level, 95% CL). On the MTM spectra and F-test, the blue (for interval 1 Pragian) and red (for interval 2 Emsian) color bars highlight the cycles that we consider significant. They are considered significant because they have strong spectral power and are visible in both intervals. The lighter red and blue color bars also display strong spectral power and are visible in both intervals, but are considered less significant because they are close to the Nyquist Frequency.

(or artifacts) between variations in the $\log(Ti)$ time series and the filtered components are rarely observed, providing robust evidence that these quasi-periodicities are real for obliquity and precession, as well as for the 10–12 k.y., 6–8 k.y., and 2.3–2.7 k.y. periods (Fig. DR2). The 2.3–2.7 k.y. cycle expression is weaker in MTM of the Emsian interval 2, so it may be not meaningful. However, it is present in the bandpass-filtered data of both intervals (Fig. DR2), mostly where the amplitude of the filtered signal is highest. For the 1.3–1.7 k.y. bandpass filter, sedimentation rate has an impact on the results. Indeed, considering the sampling interval of one sample per centimeter and the sedimentation rate of 3.5 cm/k.y. in the Emsian interval 2, there are at least five samples per 1.5 k.y. cycle; these cycles are visible in the bandpass-filtered data (Fig. DR2). In the Pragian interval 1, (sedimentation rate 1.5 cm/k.y., only two samples per 1.5 k.y. cycle), the sampling interval is not sufficient and the bandpass-filtered $\log(Ti)$ doesn't catch significant variations (Fig. DR2). We note that this 1.5 k.y. periodicity is very close to the Pleistocene Dansgaard-Oeschger cycles (Dansgaard et al., 1989). However, we refrain from making firm inferences because the periodicity is detected in only one of our records.

Finally, we assessed the stability of these quasi-periodic changes over a longer time interval by analyzing the tuned magnetic susceptibility time series of the entire Pod Barrandovem section (Da Silva et al., 2016), which spans ~5.7 m.y. In addition to the expected eccentricity-, obliquity-, and precession-related peaks, the MTM spectrum of this tuned magnetic susceptibility record (Fig. 2) shows peaks that correspond to 6–8 and 10–12 k.y. periods. Unfortunately, the sampling density (one sample every 3 k.y. on average) of the susceptibility record does not allow detection of shorter periodic variations such as those observed in our two 3 m intervals.

DISCUSSION

Millennial-scale climate changes have been linked to internal mechanisms (ice sheet dynamics, changes in the ocean-atmosphere system) or external mechanisms (harmonics and/or combination tones of primary orbital-scale cyclicity, or solar forcing). Internal mechanisms that have been held responsible for millennial-scale cyclicity in the youngest Pleistocene part of Earth history are difficult to maintain for the early Devonian, as paleogeographic conditions were fundamentally different (see also Elrick and Hinnov, 2007). Furthermore, the early Devonian is considered to have experienced a greenhouse climate. Ice sheet dynamics influence the formation of millennial-scale climatic changes only if continental ice sheets exceed a certain size threshold (McManus et al., 1999). Large continental ice sheets are highly unlikely to have existed during the early Devonian. Thus, solar forcing or combination tones of primary Milankovitch cycles are considered as plausible origins for the observed millennial-scale climate changes.

Bi-coherence spectral analysis is the most direct approach to estimate the presence of combination tones (Hagelberg et al., 1991). We applied this analysis to the entire tuned Pod Barrandovem susceptibility time series, which would include enough eccentricity, obliquity, and precession cycles to identify combination tones. Combination tones between precession and short eccentricity include: $1/100 + 1/19 = 1/16$ k.y.⁻¹. Indeed, these combination tones are visible in the bi-coherence spectrum plot: a strong peak occurs at the junction of the horizontal line at 100 k.y., the vertical line at 19 k.y., and the oblique line at 16 k.y. (circle A in Fig. 2) (see also von Dobeneck and Schmieder, 1999). The combination of the 31 k.y. obliquity and the 19 k.y. precession will generate an 11 k.y. periodic change ($1/31 + 1/19 = 1/11$ k.y.⁻¹ in the bi-coherence spectra; circle B in Fig. 2). The combination of the 16–14 k.y. horizontal line and 11 k.y. (or $1/31 + 1/11$ k.y.⁻¹) vertical line would lead to the oblique dotted line at 6 k.y. (circle C in Fig. 2). The 6 k.y. cycle on the MTM could also be related to the third harmonic of precession ($3/19 = 1/6.3$ k.y.⁻¹). The stronger peaks are located along the 100 k.y. horizontal eccentricity line (arrow α in Fig. 2), but also along the precession lines (arrows β in Fig. 2). This is also the case on the bi-spectra of the Pleistocene western equatorial Atlantic Ceara Rise

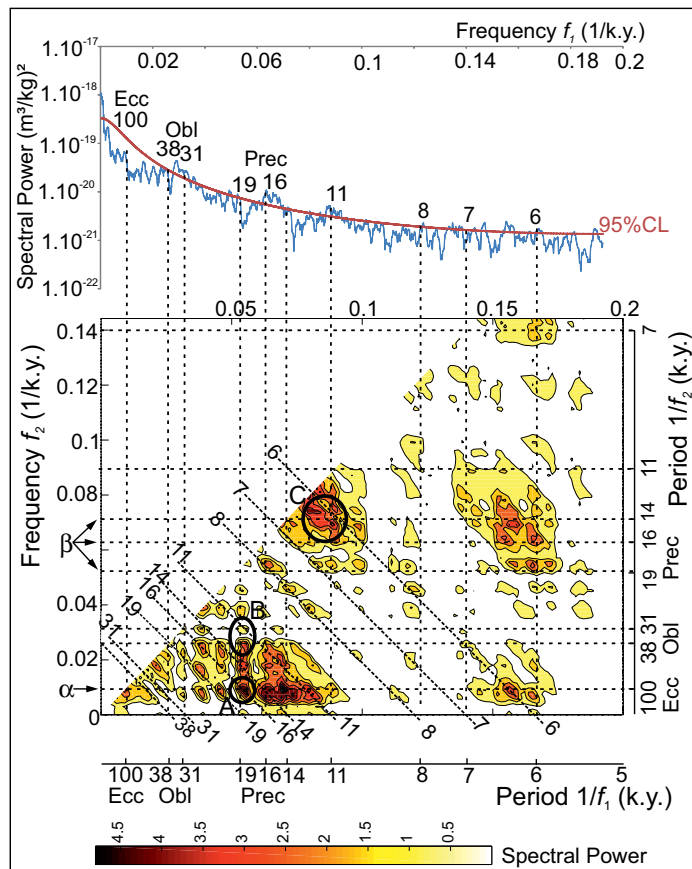


Figure 2. Spectral analysis of complete Pod Barrandovem (Czech Republic) tuned magnetic susceptibility record (from Da Silva et al., 2016). Upper part: multitaper method (MTM) spectra (four tapers) of entire tuned magnetic susceptibility record in time domain, with main frequency peaks highlighted (dotted lines) and their respective durations in k.y. and interpretations (95% confidence level [CL] marked by red line). Lower part: Bi-coherence spectrum plot of whole tuned magnetic susceptibility curve in time domain. Bi-coherence spectral analysis applied to estimate the presence of combination tones (combination of f_1 , or frequency 1, and f_2 , or frequency 2), represented by the color intensity (red color indicates strong linear coupling of frequencies). α highlights the line with the strongest linear coupling, corresponding to 100 k.y. eccentricity; β highlights the precession line. Circle A corresponds to the interaction between $1/100$ and $1/19$, giving $1/16$ k.y.⁻¹. Circle B highlights the relationship $1/31 + 1/19 = 1/11$ k.y.⁻¹. Circle C is $1/14 + 1/19 + 1/31 = 1/6$ k.y.⁻¹. Ecc—eccentricity; Obl—obliquity; Prec—precession.

records (von Dobeneck and Schmieder, 1999), with prevailing combination tones along the eccentricity and precession lines. In both cases (Devonian tropical greenhouse and Pleistocene icehouse at equatorial latitude), interactions along the obliquity lines are weaker, which would make sense in a tropical context, where obliquity has weaker influence.

So, it seems plausible from the bi-coherence spectrum that the majority of the periodic changes between 5 and 15 k.y. can be explained by precession and obliquity modulation, leading to periods of 10–12 k.y. and 6–8 k.y.

Only the second and third harmonic frequencies can represent substantial spectral power in a record (von Dobeneck and Schmieder, 1999), meaning that below 5 k.y. (corresponding to below 16 k.y./3), periods are unlikely to be combination tones of primary Milankovitch cycles. Accordingly, the 2.5 k.y. period observed in our records cannot be explained by these primary Milankovitch modulations. Variations of similar timing (1–3 k.y.) were also found at different times and in various geological settings (e.g., Draut et al., 2003; Elrick and Hinnov, 2007; Franco et al., 2012). The 2.5 k.y. period is very close to that of the ~2.4 k.y. cycle, the Hallstatt cycle, classically reported to be of heliomagnetic origin. The

Hallstatt cycle modulates the 11 yr (Schwabe) sunspot cycle (Damon and Jiríkovic, 1992). Solar forcing is considered as related to the major stable resonance of Jupiter, Saturn, Uranus, and Neptune, which would modulate the amount of cosmic rays and dust falling on Earth (Scafetta et al., 2016) and would influence climate through wind stress and humidity-aridity variations (Nederbragt and Thurow, 2005). The Hallstatt cycle has been identified in Holocene ¹⁴C and ¹⁰Be records, which are directly influenced by solar activity (Nederbragt and Thurow, 2005). In older records, the heliomagnetic origin is inferred from the correspondence in time between the recorded period and an ~2.4 k.y. period in the Pliocene (Kloosterboer-van Hove et al., 2006), Miocene (Kern et al., 2013), Eocene (Lenz et al., 2017), Permian (Franco et al., 2012), and Devonian (this work; Elrick and Hinnov, 2007).

CONCLUSIONS

The Devonian Pod Barrandovem section is characterized by millennial-scale log(Ti) changes with periodicities of 2.3–2.7, 6–8, and 10–12 k.y. obtained from two different records. A 1.5 k.y. period is also observed (similar to Dansgaard-Oeschger variations), but in only one of the two records. The omnipresence of these variations, interpreted as climate changes, during early Devonian greenhouse times, but also as detected by studies focusing on other intervals of geological history, as well as their recording in widely different settings, provides strong arguments in favor of an external origin. Bi-coherence spectra suggest that the 10–12 and 6–8 k.y. periods represent combination tones related to precession and obliquity. The 2.5 k.y. periodicity is likely related to solar forcing associated with the Hallstatt cycle.

ACKNOWLEDGMENTS

This research project was supported by the Netherlands Organization for Scientific Research (NWO, ALW grant 823.01.015WE), the Czech Science Foundation (14-18183S), and Czech institutional support (RVO 67985831). De Vleeschouwer is a postdoc in the EARTHSEQUENCING project (European Research Council Consolidator Grant awarded to Heiko Pälike). This research is part of the ICGP-652 project. We gratefully acknowledge D. Franco, one anonymous reviewer, and editor J. Parrish for their comments, which markedly improved the manuscript.

REFERENCES CITED

Alley, R.B., Clark, P.U., Keigwin, L.D., and Webb, R.S., 1999, Making sense of millennial-scale climate change, *in* Clark, P.U., et al., eds., *Mechanisms of Global Climate Change at Millennial Time Scales*: American Geophysical Union Geophysical Monograph 112, p. 385–394.

Berger, A., Loutre, M.F., and Laskar, J., 1992, Stability of the astronomical frequencies over the Earth's history for paleoclimate studies: *Science*, v. 255, p. 560–566, <https://doi.org/10.1126/science.255.5044.560>.

Berger, A., Loutre, M.F., and Mélice, J.L., 2006, Equatorial insolation: From precession harmonics to eccentricity frequencies: *Climate of the Past*, v. 2, p. 131–136, <https://doi.org/10.5194/cp-2-131-2006>.

Braun, H., Christl, M., Rahmstorf, S., Ganopolski, A., Mangini, A., Kubatzki, C., Roth, K., and Kromer, B., 2005, Possible solar origin of the 1,470-year glacial climate cycle demonstrated in a coupled model: *Nature*, v. 438, p. 208–211, <https://doi.org/10.1038/nature04121>.

Chlupáč, I., 2000, Cyclicity and duration of Lower Devonian stages: Observations from the Barrandian area, Czech Republic: *Neues Jahrbuch für Geologie und Paläontologie*, v. 215, p. 97–124, <https://doi.org/10.1127/njgpa/215/2000/97>.

Damon, P.E., and Jiríkovic, J.L., 1992, The sun as a low-frequency harmonic oscillator: *Radiocarbon*, v. 34, p. 199–205, <https://doi.org/10.1017/S003382220001362X>.

Dansgaard, W., White, J.W.C., and Johnsen, S.J., 1989, The abrupt termination of the Younger Dryas climate event: *Nature*, v. 339, p. 532–534, <https://doi.org/10.1038/339532a0>.

Da Silva, A., Hladil, J., Chadimová, L., Slavík, L., Hilgen, F.J., Bábek, O., and Dekkers, M.J., 2016, Refining the Early Devonian time scale using Milankovitch cyclicity in Lochkovian–Pragian sediments (Prague Synform, Czech Republic): *Earth and Planetary Science Letters*, v. 455, p. 125–139, <https://doi.org/10.1016/j.epsl.2016.09.009>.

de Winter, N.J., Zeeden, C., and Hilgen, F.J., 2014, Low-latitude climate variability in the Heinrich frequency band of the Late Cretaceous greenhouse world: *Climate of the Past*, v. 10, p. 1001–1015, <https://doi.org/10.5194/cp-10-1001-2014>.

Draut, A.E., Raymo, M.E., McManus, J.F., and Oppo, D.W., 2003, Climate stability during the Pliocene warm period: *Paleoceanography*, v. 18, 1078, <https://doi.org/10.1029/2003PA000889>.

Du, M., 2013, Comparing nonlinear climate responses to orbital-insolation during the early Miocene and Pleistocene: A bicoherence study [M.S. thesis]: Madison, The University of Wisconsin, 55 p.

Elrick, M., and Hinnov, L.A., 2007, Millennial-scale paleoclimate cycles recorded in widespread Paleozoic deeper water rhythmites of North America: *Paleoceanography, Palaeoclimatology, Palaeoecology*, v. 243, p. 348–372, <https://doi.org/10.1016/j.palaeo.2006.08.008>.

Franco, D.R., Hinnov, L.A., and Ernesto, M., 2012, Millennial-scale climate cycles in Permian–Carboniferous rhythmites: Permanent feature throughout geologic time?: *Geology*, v. 40, p. 19–22, <https://doi.org/10.1130/G32338.1>.

Hagelberg, T., Pisiás, N., and Elgar, S., 1991, Linear and nonlinear couplings between orbital forcing and the marine $\delta^{18}\text{O}$ record during the Late Neogene: *Paleoceanography*, v. 6, p. 729–746, <https://doi.org/10.1029/91PA02281>.

Heinrich, H., 1988, Origin and consequences of cyclic ice rafting in the Northeast Atlantic Ocean during the past 130,000 years: *Quaternary Research*, v. 29, p. 142–152, [https://doi.org/10.1016/0033-5894\(88\)90057-9](https://doi.org/10.1016/0033-5894(88)90057-9).

Hladil, J., Cejchan, P., Bábek, O., Koptíková, L., Navrátil, T., and Kubínová, P., 2010, Dust—A geology-orientated attempt to reappraise the natural components, amounts, inputs to sediment, and importance for correlation purposes: *Geologica Belgica*, v. 13, p. 367–384.

Joachimski, M.M., Breisig, S., Buggisch, W., Talent, J.A., Mawson, R., Gereke, M., Morrow, J.R., Day, J., and Weddige, K., 2009, Devonian climate and reef evolution: Insights from oxygen isotopes in apatite: *Earth and Planetary Science Letters*, v. 284, p. 599–609, <https://doi.org/10.1016/j.epsl.2009.05.028>.

Kern, A.K., Harzhauser, M., Soliman, A., Piller, W.E., and Mandic, O., 2013, High-resolution analysis of upper Miocene lake deposits: Evidence for the influence of Gleissberg-band solar forcing: *Paleoceanography, Palaeoclimatology, Palaeoecology*, v. 370, p. 167–183, <https://doi.org/10.1016/j.palaeo.2012.12.005>.

Kloosterboer-van Hove, M.L., Steenbrink, J., Visscher, H., and Brinkhuis, H., 2006, Millennial-scale climatic cycles in the Early Pliocene pollen record of Ptolemais, northern Greece: *Paleoceanography, Palaeoclimatology, Palaeoecology*, v. 229, p. 321–334, <https://doi.org/10.1016/j.palaeo.2005.07.002>.

Lenz, O.K., Wilde, V., and Riegel, W., 2017, ENSO- and solar-driven sub-Milankovitch cyclicity in the Palaeogene greenhouse world: High-resolution pollen records from Eocene Lake Messel, Germany: *Journal of the Geological Society*, v. 174, p. 110–128, <https://doi.org/10.1144/jgs2016-046>.

MacAyeal, D.R., 1993, Binge/purge oscillations of the Laurentide Ice Sheet as a cause of the North Atlantic's Heinrich events: *Paleoceanography*, v. 8, p. 775–784, <https://doi.org/10.1029/93PA02200>.

MacLean, W.H., Bonavia, F.F., and Sanna, G., 1997, Argillite debris converted to bauxite during karst weathering: Evidence from immobile element geochemistry at the Olmedo Deposit, Sardinia: *Mineralium Deposita*, v. 32, p. 607–616, <https://doi.org/10.1007/s001260050126>.

McManus, J.F., Oppo, D.W., and Cullen, J.L., 1999, A 0.5-million-year record of millennial-scale climate variability in the North Atlantic: *Science*, v. 283, p. 971–975, <https://doi.org/10.1126/science.283.5404.971>.

Meyers, S.R., 2014, astrochron: An R package for astrochronology, Version 7.0: <http://cran.r-project.org/package=astrochron>.

Nederbragt, A.J., and Thurow, J., 2005, Geographic coherence of millennial-scale climate cycles during the Holocene: *Paleoceanography, Palaeoclimatology, Palaeoecology*, v. 221, p. 313–324, <https://doi.org/10.1016/j.palaeo.2005.03.002>.

Scafetta, N., Milani, F., Bianchini, A., and Ortolani, S., 2016, On the astronomical origin of the Hallstatt oscillation found in radiocarbon and climate records throughout the Holocene: *Earth-Science Reviews*, v. 162, p. 24–43, <https://doi.org/10.1016/j.earscirev.2016.09.004>.

Slavík, L., Valenzuela-Ríos, J.I., Hladil, J., Chadimová, L., Liao, J.-C., Hušková, A., Calvo, H., and Hrstka, T., 2016, Warming or cooling in the Pragian? Sedimentary record and petrophysical logs across the Lochkovian–Pragian boundary in the Spanish Central Pyrenees: *Paleoceanography, Palaeoclimatology, Palaeoecology*, v. 449, p. 300–320, <https://doi.org/10.1016/j.palaeo.2016.02.018>.

Thomson, D.J., 1982, Spectrum estimation and harmonic analysis: *Proceedings of the IEEE*, v. 70, p. 1055–1096, <https://doi.org/10.1109/PROC.1982.12433>.

Torrence, C., and Compo, G.P., 1998, A practical guide to wavelet analysis: *Bulletin of the American Meteorological Society*, v. 79, p. 61–78, [https://doi.org/10.1175/1520-0477\(1998\)079<0061:APGTWA>2.0.CO;2](https://doi.org/10.1175/1520-0477(1998)079<0061:APGTWA>2.0.CO;2).

von Dobeneck, T., and Schmieder, F., 1999, Using rock magnetic proxy records for orbital tuning and extended time series analyses into the super- and sub-Milankovitch bands, *in* Fischer, G., and Wefer, G., eds., *Use of Proxies in Paleoclimatology: Examples from the South Atlantic*: Berlin Heidelberg, Springer-Verlag, p. 601–633, https://doi.org/10.1007/978-3-642-58646-0_25.

Wara, M.W., Ravelo, A.C., and Revenaugh, J.S., 2000, The pacemaker always rings twice: *Paleoceanography*, v. 15, p. 616–624, <https://doi.org/10.1029/2000PA000500>.

Printed in USA